

# Numerical simulations of semi-linear Klein-Gordon equations in the de Sitter spacetime with structure preserving scheme

Takuya Tsuchiya<sup>\*1</sup> and Makoto Nakamura<sup>2</sup>

<sup>1</sup>Center for Liberal Arts and Sciences, Hachinohe Institute of Technology, Japan,

<sup>2</sup>Faculty of Science, Yamagata University, Japan,

March 18, 2022

## Abstract

We perform some simulations of the Klein-Gordon equation in the de Sitter spacetime. We reported the stable and high-precision numerical results of the equation using the structure preserving scheme (SPS) in an earlier publication (Tsuchiya and Nakamura in *J. Comput. Appl. Math.* 361: 396–412, 2019). To investigate the factors of the stability and accuracy of the simulations with SPS, we perform some simulations with three discretized formulations. The first formulation is the discretized equations with SPS, the second is with SPS which replaced the second derivative term as the standard difference, and the third is with SPS which replaced the non-linear term as the standard expression. As a result, the above two replacements in SPS are found to be effective for stable and high-precision simulations.

## 1 Introduction

It is necessary of stable and high-precision numerical simulations to understand the natural phenomena and the social phenomena in details. To realize it, the numerical methods such as the discretizations need to be in a mathematically guaranteed format because the numerical errors are mainly occurred in the process of the discretizations. For numerical schemes of the partial differential equations, there are several well-known methods such as the Crank-Nicolson scheme and the Runge-Kutta scheme. Since the simulations with these schemes often have large numerical errors for the nonlinear equations (e.g., [1]), the suitable schemes have been suggested. One of the schemes is the structure preserving scheme (SPS) [2]. This scheme conserves some structures of the continuous level, and thus allows for stable and high-precision numerical simulations.

In this paper, we review the discretized equations of the semi-linear Klein-Gordon equation in the de Sitter spacetime with SPS and perform some simulations to confirm the stability and the numerical accuracy. For investigations of Klein-Gordon equation in the de Sitter spacetime, analytical researches [5, 6, 7, 8, 9] and numerical researches [10, 1] are reported. In [1], we reported some stable and high-precision numerical results with SPS. There are some differences between the standard discretized equation and the discretized equation with SPS. In this paper, we investigate the effect of these differences on the stability and accuracy of the simulations.

The structure of this paper is as follows. We review the canonical equation of the Klein-Gordon equation in the de Sitter spacetime in Sec. 2 and the discretized equation with SPS in Sec. 3. In Sec. 4, we perform some simulations for confirmation of the stability and accuracy of the discretized equation. We summarize this paper in Sec. 5. In this paper, the indices such as  $(i, j, k, \dots)$  run from 1 to 3. We use the Einstein convention of summation of repeated up-down indices.

## 2 Canonical formulation of Klein-Gordon equation in de Sitter spacetime

The Klein-Gordon equation is

$$\partial_t^2 \phi + 3H\partial_t \phi - e^{-2Ht} \delta^{ij} (\partial_i \partial_j \phi) + m^2 \phi + \lambda |\phi|^{p-1} \phi = 0, \quad (1)$$

---

<sup>\*</sup>t-tsuchiya@hi-tech.ac.jp

where  $\phi$  is the field variable,  $H$  is the Hubble constant,  $\delta^{ij}$  denotes the Kronecker delta,  $m$  is its mass,  $\lambda$  is a Boolean parameter, and  $p$  is an integer of 2 or more. For performing the simulations of Eq. (1), we often recast a system of the first order differential equations. There are several systems, we make a canonical formulation of the equations. This is because the canonical formulation has the total Hamiltonian, and this value is a criteria to confirm the simulations are successful.

The Hamiltonian density of Eq. (1) is defined

$$\mathcal{H} = \frac{1}{2}e^{-3Ht}\psi^2 + \frac{1}{2}e^{Ht}\delta^{ij}(\partial_i\phi)(\partial_j\phi) + m^2e^{3Ht}\phi^2 + \frac{\lambda}{p+1}e^{3Ht}|\phi|^{p+1}, \quad (2)$$

where  $\psi$  is the conjugate momentum of  $\phi$ . Then, by the canonical equations of  $\mathcal{H}$  the evolution equations are given as

$$\partial_t\phi = e^{-3Ht}\psi, \quad (3)$$

$$\partial_t\psi = e^{Ht}\delta^{ij}(\partial_j\partial_i\phi) - m^2e^{3Ht}\phi - \lambda e^{3Ht}|\phi|^{p-1}\phi. \quad (4)$$

The total Hamiltonian  $H_C$  is defined as

$$H_C \equiv \int \mathcal{H} d^3x, \quad (5)$$

then the time derivative of  $H_C$  is

$$\partial_t H_C = 3HH_C - H(3e^{-3Ht}\psi^2 + e^{Ht}\delta^{ij}(\partial_i\phi)(\partial_j\phi)). \quad (6)$$

Note that  $H$  is the Hubble constant and  $H_C$  is the total Hamiltonian. If  $H = 0$ ,  $\partial_t H_C = 0$ . Thus, the system has conservative property. On the other hand, for the case of  $H \neq 0$ , it is not conserved  $H_C$  in general. For the case of  $H \neq 0$ , we defined the value

$$\tilde{H}_C(t) \equiv H_C(t) - \int_0^t \partial_t H_C(s) ds. \quad (7)$$

$\tilde{H}_C$  satisfies identically  $\partial_t \tilde{H}_C = 0$ . We call the value  $\tilde{H}_C$  as the modified total Hamiltonian here after. To confirm the precision of the simulations, we monitor the  $H_C$  in the flat spacetime such as  $H = 0$ , and  $\tilde{H}_C$  in the non-flat spacetime such as  $H = 10^{-3}$ . If  $H_C$  in the flat spacetime or  $\tilde{H}_C$  in the non-flat spacetime is unchanged in the evolution, we determine the simulations are successful. In details, the smaller the change in the value of  $H_C$  or  $\tilde{H}_C$  in the evolution means more accurate numerical calculations.

### 3 Discretizations equations of Klein Gordon equation in the de Sitter spacetime

The main factor of the numerical errors is caused in the process of the discretizations of the equations. By using SPS as the discretized scheme, we can reduce the errors. In this Section, we review the discretized equations of the Klein-Gordon equations in the de Sitter spacetime.

The discrete Hamiltonian density is defined as

$$\begin{aligned} \mathcal{H}_{(k)}^{(\ell)} = & \frac{1}{2}e^{-3Ht_\ell}(\psi_{(k)}^{(\ell)})^2 + \frac{1}{2}e^{Ht_\ell}\delta^{ij}(\hat{\delta}_i^{(1)}\phi_{(k)}^{(\ell)})(\hat{\delta}_j^{(1)}\phi_{(k)}^{(\ell)}) + m^2e^{3Ht_\ell}(\phi_{(k)}^{(\ell)})^2 \\ & + \frac{\lambda}{p+1}e^{3Ht_\ell}|\phi_{(k)}^{(\ell)}|^{p+1}, \end{aligned} \quad (8)$$

and the discretized equations of Eqs. (3)–(4) are

$$\frac{\phi_{(k)}^{(\ell+1)} - \phi_{(k)}^{(\ell)}}{\Delta t} = \frac{1}{4}(e^{-3Ht_{\ell+1}} + e^{-3Ht_\ell})(\psi_{(k)}^{(\ell+1)} + \psi_{(k)}^{(\ell)}), \quad (9)$$

$$\begin{aligned} \frac{\psi_{(k)}^{(\ell+1)} - \psi_{(k)}^{(\ell)}}{\Delta t} = & \frac{1}{4}(e^{Ht_{\ell+1}} + e^{Ht_\ell})\delta^{ij}\hat{\delta}_j^{(1)}\hat{\delta}_i^{(1)}(\phi_{(k)}^{(\ell+1)} + \phi_{(k)}^{(\ell)}) \\ & - \frac{m^2}{4}(e^{3Ht_{\ell+1}} + e^{3Ht_\ell})(\phi_{(k)}^{(\ell+1)} + \phi_{(k)}^{(\ell)}) \\ & - \frac{\lambda}{2(p+1)}(e^{3Ht_{\ell+1}} + e^{3Ht_\ell})\frac{|\phi_{(k)}^{(\ell+1)}|^{p+1} - |\phi_{(k)}^{(\ell)}|^{p+1}}{\phi_{(k)}^{(\ell+1)} - \phi_{(k)}^{(\ell)}}, \end{aligned} \quad (10)$$

respectively, where the upper index with parenthesis such as  $(\ell)$  is time index and the lower index with parenthesis such as  $(k)$  is spatial grid index.  $\widehat{\delta}_i^{(1)}$  is the discrete operator defined as

$$\widehat{\delta}_i^{(1)} u_{(k)}^{(\ell)} = \frac{u_{(k+1)}^{(\ell)} - u_{(k-1)}^{(\ell)}}{2\Delta x^i} \quad (11)$$

where  $\Delta x^i = (\Delta x, \Delta y, \Delta z)$  is the spatial mesh width. There are two features in Eq. (10). First, the second order derivative is expressed as  $\widehat{\delta}_j^{(1)} \widehat{\delta}_i^{(1)}$ . Generally, the discrete operator of the second order derivative is usually defined as

$$\widehat{\delta}_{ij}^{(2)} u_{(k)}^{(\ell)} = \begin{cases} \frac{u_{(k)}^{(\ell+1)} - 2u_{(k)}^{(\ell)} + u_{(k)}^{(\ell-1)}}{(\Delta x^i)^2}, & (j = i) \\ \widehat{\delta}_j^{(1)} \widehat{\delta}_i^{(1)} u_{(k)}^{(\ell)}. & (j \neq i) \end{cases} \quad (12)$$

For the case of  $i = j$ ,  $\widehat{\delta}_{ij}^{(2)} u_{(k)}^{(\ell)} \neq \widehat{\delta}_i^{(1)} \widehat{\delta}_j^{(1)} u_{(k)}^{(\ell)}$ . Second, the expression of the nonlinear term which is the last term of the right hand side in Eq. (10) is not usual. Generally, the expression expected from (4) is  $-\lambda e^{3Ht_\ell} |\phi_{(k)}^{(\ell)}|^{p-1} \phi_{(k)}^{(\ell)}$ . These differences in the simulations are shown in Sec. 4.

## 4 Numerical simulations

In this Section, we perform some simulations for confirmation of the stability and the accuracy of SPS. To compare the stability and the accuracy, we perform simulations with three formulations of the discrete Klein-Gordon equation in the de Sitter spacetime. The first formulation (Form I) is Eqs. (9)–(10). Form I is SPS. The second formulation (Form II) is Eq. (9) and

$$\begin{aligned} \frac{\psi_{(k)}^{(\ell+1)} - \psi_{(k)}^{(\ell)}}{\Delta t} &= \frac{1}{4} (e^{Ht_{\ell+1}} + e^{Ht_\ell}) \delta^{ij} \widehat{\delta}_{ij}^{(2)} (\phi_{(k)}^{(\ell+1)} + \phi_{(k)}^{(\ell)}) \\ &\quad - \frac{m^2}{4} (e^{3Ht_{\ell+1}} + e^{3Ht_\ell}) (\phi_{(k)}^{(\ell+1)} + \phi_{(k)}^{(\ell)}) \\ &\quad - \frac{\lambda}{2(p+1)} (e^{3Ht_{\ell+1}} + e^{3Ht_\ell}) \frac{|\phi_{(k)}^{(\ell+1)}|^{p+1} - |\phi_{(k)}^{(\ell)}|^{p+1}}{\phi_{(k)}^{(\ell+1)} - \phi_{(k)}^{(\ell)}}. \end{aligned} \quad (13)$$

The difference between Eq. (10) and Eq. (13) is the difference term of the second order derivative. The third formulation (Form III) is Eq. (9) and

$$\begin{aligned} \frac{\psi_{(k)}^{(\ell+1)} - \psi_{(k)}^{(\ell)}}{\Delta t} &= \frac{1}{4} (e^{Ht_{\ell+1}} + e^{Ht_\ell}) \delta^{ij} \widehat{\delta}_i^{(1)} \widehat{\delta}_j^{(1)} (\phi_{(k)}^{(\ell+1)} + \phi_{(k)}^{(\ell)}) \\ &\quad - \frac{m^2}{4} (e^{3Ht_{\ell+1}} + e^{3Ht_\ell}) (\phi_{(k)}^{(\ell+1)} + \phi_{(k)}^{(\ell)}) \\ &\quad - \frac{\lambda}{8} (e^{3Ht_{\ell+1}} + e^{3Ht_\ell}) |\phi_{(k)}^{(\ell+1)} + \phi_{(k)}^{(\ell)}|^{p-1} (\phi_{(k)}^{(\ell+1)} + \phi_{(k)}^{(\ell)}). \end{aligned} \quad (14)$$

The difference between Eq. (10) and Eq. (14) is the expression of the discrete nonlinear term.

The simulation settings are followings.

- Initial condition:  $\phi_0 = A \cos(2\pi x)$ ,  $\psi_0 = 2\pi A \sin(2\pi x)$  and  $A = 4$ .
- Numerical domains:  $0 \leq x \leq 1$ ,  $0 \leq t \leq 1000$ .
- Boundary condition: periodic.
- Grids:  $\Delta x = 1/200$  and  $\Delta t = 1/500$ .
- The mass  $m = 1$ , and the Boolean parameter of the nonlinear term:  $\lambda = 1$ .
- The number of exponent in the nonlinear term:  $p = 2, 3, 4, 5, 6$ .
- The Hubble constant  $H = 0, 10^{-3}$ .

## 4.1 Flat spacetime

We perform some simulations of the three formulations in the flat spacetime  $H = 0$ . In Fig. 1, we show the total Hamiltonian  $H_C$  for each the number of exponent  $p$  in the nonlinear term. The top-left panel is drawn with Form I,

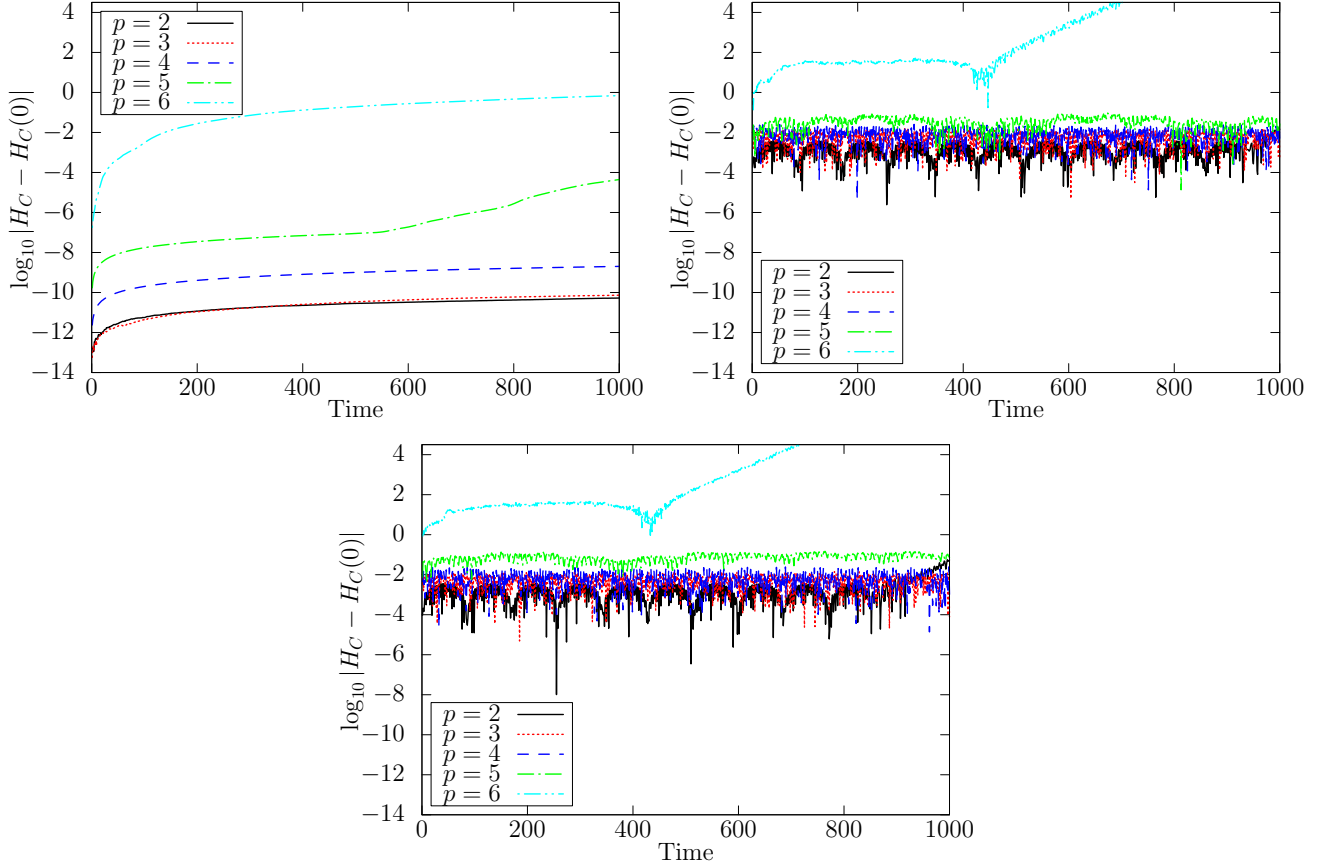


Figure 1: Differences between the total Hamiltonian  $H_C$  and that of the initial value  $H_C(0)$  in the Hubble constant as  $H = 0$ . The horizontal axis is time, and the vertical axis is  $\log_{10} |H_C - H_C(0)|$ . The left top panel is drawn with Form I, the right top panel is with Form II, and the bottom panel is with Form III.

the top-right panel is drawn with Form II, and the bottom panel is drawn with Form III. The values of  $|H_C - H_C(0)|$  mean the numerical errors. We see the values of the top-right panel and bottom panel are larger than that of the top-left panel for each  $p$ . Thus the simulations with Form I are more accurate than the others. The values of  $p = 5$  and  $p = 6$  are larger than the others for each panel.

Then we show  $\phi$  of  $p = 5$  and  $p = 6$  in Fig. 2. The top panels are drawn with Form I, the middle panels are with Form II, and the bottom panels are with Form III. The left panels are drawn with the number of exponent value setting as  $p = 5$  and the right panels are with  $p = 6$ . We see the simulations of the middle-right panel and bottom-right panel are failed in  $t \geq 800$ . On the other hand, the simulation of the top right panel is successful until  $t = 1000$ . Thus we determine the simulation of Form I is more stable than that of the other formulations. Moreover, in Fig. 1, we see the values of  $|H_C - H_C(0)|$  for  $p = 5$  in the case of Form I are smaller than the values of Form II and Form III. For the case of  $p = 6$ , the result is the same. For these reasons, although the vibrations are occurred  $t \geq 700$  in top-left panel and  $t \geq 200$  in top-right panel, the simulations of Form I are performed more stable and accurate than the other formulations.

## 4.2 Curved spacetime

Here we perform some simulations with the same settings as in Sec. 4.1 except for the Hubble constant. This time we set the Hubble constant as  $H = 10^{-3}$ .

We show the differences of the modified total Hamiltonian  $\tilde{H}_C$  and that of the initial value  $\tilde{H}_C(0)$  in Fig. 3. The top-left panel is drawn with Form I, the top-right panel is drawn with Form II, and the bottom panel is drawn with

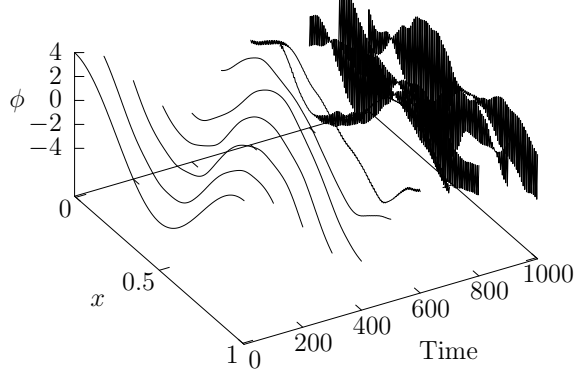
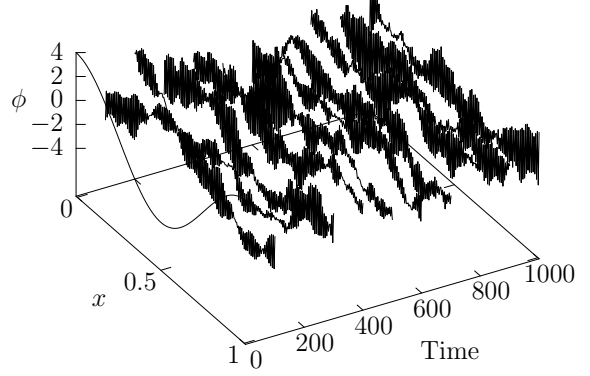
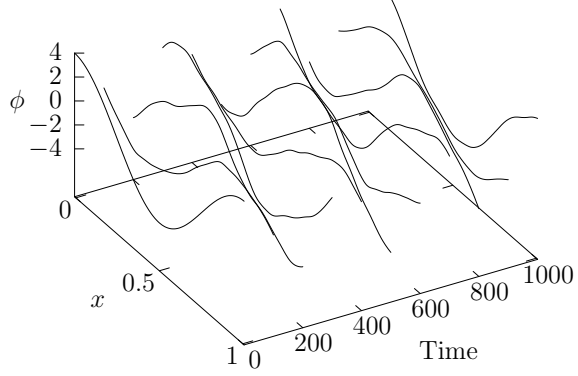
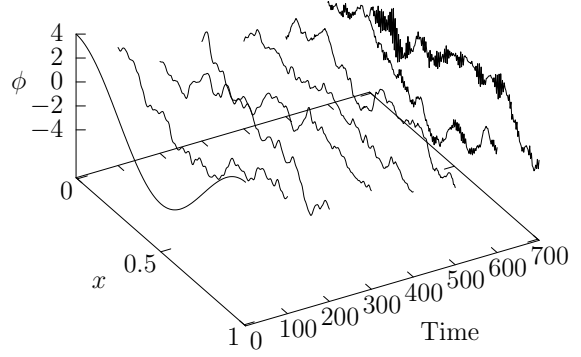
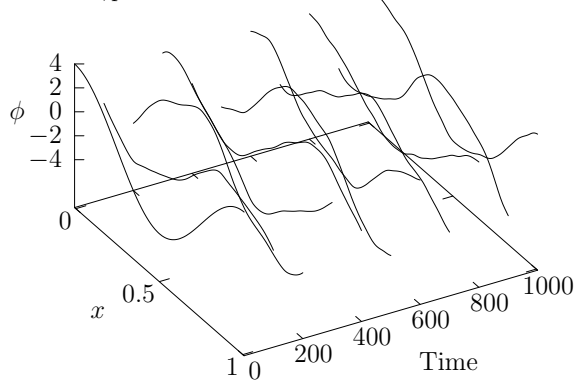
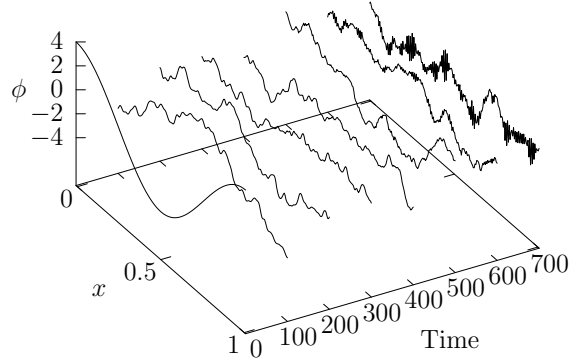
Form I,  $p = 5$ Form I,  $p = 6$ Form II,  $p = 5$ Form II,  $p = 6$ Form III,  $p = 5$ Form III,  $p = 6$ 

Figure 2:  $\phi$  with the number of exponent value  $p$  as 5 and 6. The top panels are drawn with Form I, the middle panels are with Form II, and the bottom panels are with Form III. The left panels are drawn for the case of  $p = 5$  and the right panels are for the case of  $p = 6$ . The vibrations are occurred  $t \geq 700$  in the top-left panel and  $t \geq 200$  in the top-right panel. For the middle-right panel and bottom-right panel, the simulations are failed  $t \geq 800$ .

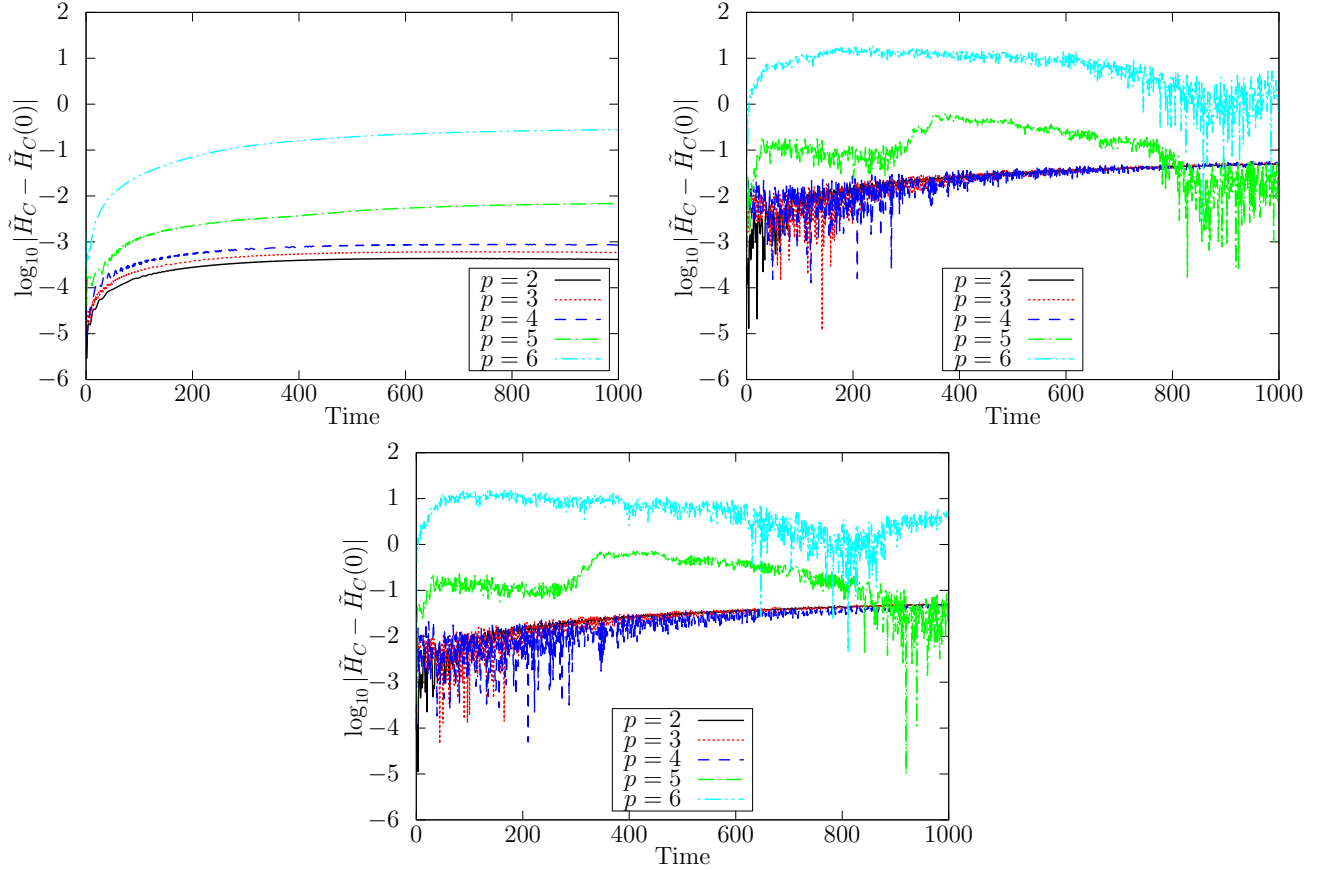


Figure 3: Differences between the modified total Hamiltonian  $\tilde{H}_C(t)$  and that of the initial value  $\tilde{H}_C(0)$  in the Hubble constant as  $H = 10^{-3}$ . The horizontal axis is time, and the vertical axis is  $\log_{10} |\tilde{H}_C - \tilde{H}_C(0)|$ . The top-left panel is drawn with Form I, the top-right panel is with Form II, and the bottom panel is with Form III.

Form III. As the same as the case in Sec. 4.1, we see the values of  $p = 5$  and  $p = 6$  are larger than the others for each panel. For each number of  $p$ , the values of the top-left panel are smaller than the others. Thus, the accuracy with Form I is better than the other formulations.

Fig. 4 is the same as Fig. 2 except for the value of the Hubble constant. Comparison with Fig. 2 and Fig. 4, the vibrations are not appeared in the top-left panel in Fig. 4, and the simulations continue until  $t = 1000$  in the middle-right panel and the bottom-right panel in Fig. 4. For these results, the positiveness of the Hubble constant make stable and accurate simulations. We note that the same descriptions are in [1].

## 5 Summary

We investigated the factors affecting the stability and the accuracy of simulations of the Klein-Gordon equation in the de Sitter spacetime using the structure preserving scheme (SPS). We reviewed the canonical formulation of the equation and that of the discretized equation with SPS. In order to investigate the effective terms on the stability and the accuracy in the discretized equations, we compared some simulations with three formulations of the discretized equations. The first is the discretized equation using SPS reported in [1]. The second is using SPS, but replaced the second-order derivative term with a standard difference term. The third is using SPS, but replaced the nonlinear term with a standard discrete term. We monitored the total Hamiltonian or the modified one to see the accuracy of the simulations. Then the accuracy and the stability of the simulations with the first formulation is better than the second and third formulations. And we confirmed that the simulations with positive value of the Hubble constant are more stable and accurate than the ones in the flat spacetime.

The relationship between the accuracy and difference term of the second-order derivative term is similar to the result in the Maxwell equation case [11]. By using the difference term of the second-order derivative used in this paper, it is expected that numerical simulations of general wave-type partial differential equations are performed stably and accurately.

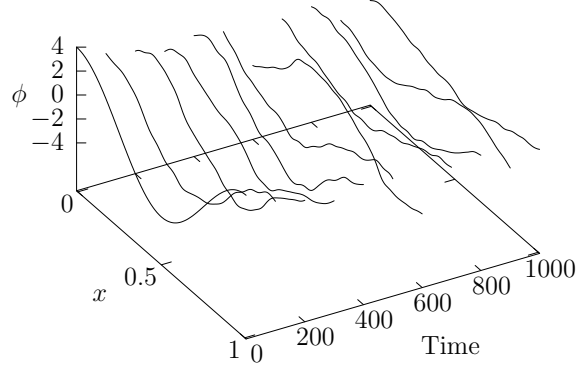
## Acknowledgments

T.T. and M.N. were partially supported by JSPS KAKENHI Grant Number 21K03354. T.T. was partially supported by JSPS KAKENHI Grant Number 20K03740, and Grant for Basic Science Research Projects from The Sumitomo Foundation. M.N. was partially supported by JSPS KAKENHI Grant Number 16H03940.

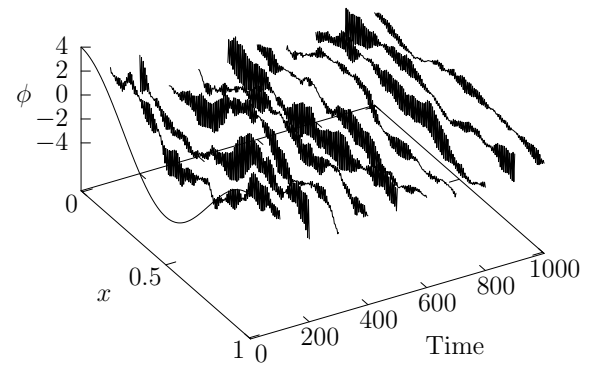
## References

- [1] Tsuchiya, T., Nakamura, M.: On the numerical experiments of the Cauchy problem for semi-linear Klein-Gordon equations in the de Sitter spacetime. *J. Comput. Appl. Math.* **361**, 396–412 (2019)
- [2] Furihata, D., Matsuo, T.: *Discrete Variational Derivative Method*. CRC Press/Taylor & Francis, London (2010)
- [3] Furihata, D.: Finite difference schemes for  $\frac{\partial u}{\partial t} = (\frac{\partial}{\partial x})^\alpha \frac{\delta G}{\delta u}$  that inherit energy conservation or dissipation property. *J. Comput. Phys.* **156**, 181–205 (1999)
- [4] Tsuchiya, T., Yoneda, G.: Constructing of constraint preserving scheme for Einstein equations. *JSIAM Letters* **9**, 57–60 (2016)
- [5] Yagdjian, K., Galstian, A.: Fundamental solutions for the Klein–Gordon equation in de Sitter spacetime. *Comm. Math. Phys.* **285** (1), 293–344 (2009)
- [6] Yagdjian, K.: The semilinear Klein–Gordon equation in de Sitter spacetime. *Discrete Contin. Dyn. Syst. Ser. S* **2** (3), 679–696 (2009)
- [7] Yagdjian, K.: Global solutions of semilinear system of Klein–Gordon equations in de Sitter spacetime. *Progress in Partial Differential Equations*, Springer, Proceedings in Mathematics & Statistics **44**, 409–444 (2013)
- [8] Nakamura, M.: The Cauchy problem for semi-linear Klein–Gordon equations in de Sitter spacetime. *J. Math. Anal. Appl.* **410** (1), 445–454 (2014)

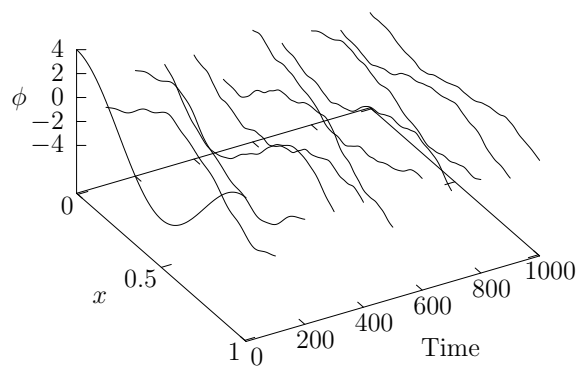
Form I,  $p = 5$



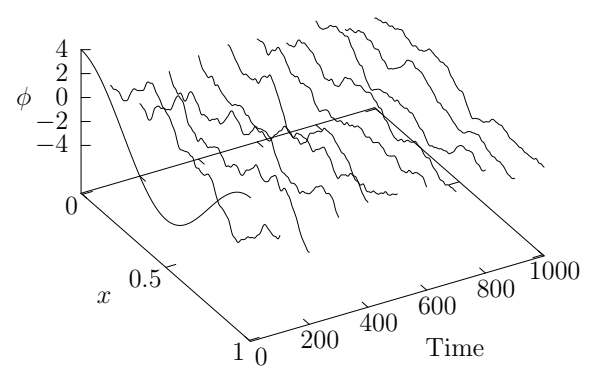
Form I,  $p = 6$



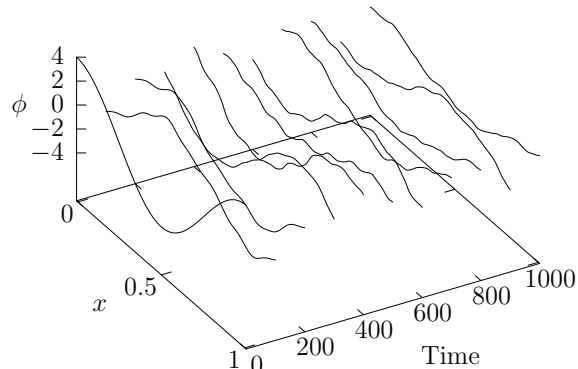
Form II,  $p = 5$



Form II,  $p = 6$



Form III,  $p = 5$



Form III,  $p = 6$

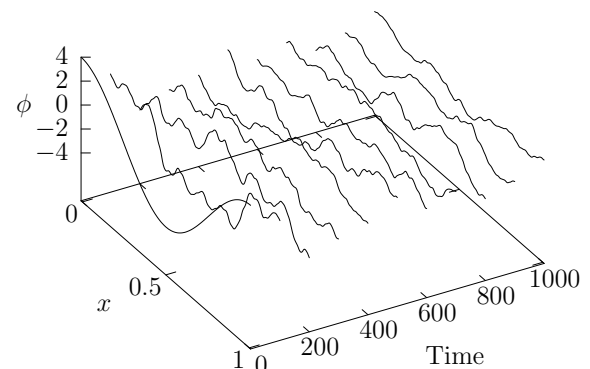


Figure 4: As the same as Fig. 2 except for the value of the Hubble constant. The value of the Hubble constant is  $10^{-3}$ .

- [9] Nakamura, M.: The Cauchy problem for the Klein–Gordon equation under the quartic potential in the de Sitter spacetime. *J. Math. Phys.* **62**, 121509 (2021)
- [10] Yazici, M. and Şengül, S.: Approximate solutions to the nonlinear Klein-Gordon equation in de Sitter spacetime. *Open Physics* **14** (1), 314–320 (2016)
- [11] Tsuchiya, T., Yoneda G.: Constraint-Preserving Scheme for Maxwell’s Equations. *arXiv:gr-qc:1610.04370* (2016)